Asymmetric Stationary Lasing Patterns in 2D Symmetric Microcavities

Takahisa Harayama,[1] Takehiro Fukushima,[2] Satoshi Sunada,[1,3] and Kensuke S. Ikeda[3]

[1]*ATR Adaptive Communications Research Laboratories, 2-2-2 Hikaridai Seika-cho, Soraku-gun, Kyoto 619-0228, Japan*
[2]*Department of Communication Engineering, Okayama Prefectural University, 111 Kuboki, Soja, Okayama 719-1197, Japan*
[3]*Department of Physics, Ritsumeikan University, 1916 Noji-cho, Kusatsu, Shiga 525, Japan*

Locking of two resonance modes of different symmetry classes and different frequencies in 2D resonant microcavity lasers is investigated by using a nonlinear dynamical model. The patterns of stationary lasing states and far fields are asymmetric in spite of the symmetric shape of the resonant microcavity. The corresponding phenomenon is actually observed in the experiment of a 2D semiconductor microcavity laser diode.

Advances in processing technology have made it possible to make new types of 2D microcavity lasers with potential applications as light sources and other key components in integrated optical circuits. 2D microcavity lasers also present a practical and versatile stage for fundamental research of morphological effects of resonant cavities on laser operation [1–5]. Lasing in whispering gallery modes has been realized in microdisks [6–9]. Lasing has also been demonstrated in deformed microdisks which trade off the efficiency of optical confinement to obtain sufficiently strong or directional output [3,4]. When the disk shape is deformed, the cavity can become *partially chaotic*, in the sense that some ray trajectories are chaotic. However, the relation between cavity shape and optical confinement of low loss modes in partially chaotic cavities can still be described in terms of ray trajectories, and well understood from the viewpoint of ray-wave correspondence and quantum chaos [3–5]. Recently nonlinear dynamical simulations have also shown that stable lasing in a *fully chaotic* cavity is possible in spatially chaotic pattern of the light field of a resonance mode [10].

All of the previous works have focused on the morphological effects on *single-mode* lasing in 2D microcavities. In this Letter, we present the dynamics of *two-mode* lasing in 2D microcavities for the first time. The route to locking of two modes is shown theoretically and numerically. We also show that locking of two modes is actually observed in the experiments of a 2D semiconductor microcavity laser.

It is important to note that most of the 2D microcavities previously studied are symmetric with respect to the *x* and *y* axes such as an elliptic cavity. Then the resonance modes are divided into four symmetry classes: $\psi_{ab}(-x, y) = a\psi_{ab}(x, y)$ and $\psi_{ab}(x, -y) = b\psi_{ab}(x, y)$ with the parities $a \in \{+, -\}$ and $b \in \{+, -\}$. We show that when two modes of different symmetry classes are locked, the pattern of a stationary lasing state becomes asymmetric.

The dynamics of the slowly varying envelope of the electric field $\tilde{E}$, the polarization field $\tilde{\rho}$, and the population inversion component W is described by the Schrödinger-Bloch model [10–12] when the 2D microcavity is confined in the waveguide which is wide in the *xy* directions and thin in the *z* direction, and the refractive index suddenly changes on the edge of the cavity;

$$\frac{\partial \tilde{E}}{\partial t} = \frac{i}{2}\left(\nabla_{xy}^2 + \frac{n^2}{n_{in}^2}\right)\tilde{E} - \alpha_L(x, y)\tilde{E} + \frac{2\pi N\kappa\hbar}{\epsilon}\tilde{\rho}, \quad (1)$$

$$\frac{\partial \tilde{\rho}}{\partial t} = -i\Delta_0\tilde{\rho} - \tilde{\gamma}_\perp\tilde{\rho} + \tilde{\kappa}W\tilde{E}, \quad (2)$$

$$\frac{\partial W}{\partial t} = -\tilde{\gamma}_\parallel(W - W_\infty) - 2\tilde{\kappa}(\tilde{E}\tilde{\rho}^* + \tilde{E}^*\tilde{\rho}), \quad (3)$$

where space and time are made dimensionless by the scale transformation $(n_{in}\omega_s x/c, n_{in}\omega_s y/c) \rightarrow (x, y)$ and $t\omega_s \rightarrow t$, respectively. In the above, ω_0 is the transition frequency of the two-level medium while ω_s is the oscillation frequency of the light field slightly different from ω_0, and the refractive index n equals n_{in} inside the cavity and n_{out} outside the cavity, and $\alpha_L(x, y)$ is the linear absorption coefficient, which is the constant α_L inside the cavity and zero outside the cavity. The two (dimensionless) relaxation parameters $\tilde{\gamma}_\perp$ and $\tilde{\gamma}_\parallel$ are the transversal relaxation rate and the longitudinal relaxation rate, respectively, and W_∞ is the external pumping parameter. $\tilde{\kappa}$ is the dimensionless coupling strength, $\kappa = \tilde{\kappa}/\omega_0$ and $\Delta_0 = \omega_0/\omega_s - 1$.

First, we assume the refractive index is extremely high in order to analyze the Schrödinger-Bloch model theoretically. Then the cavity modes become the bound states U_n satisfying the Helmholtz equation inside the cavity,

$$-\left(\nabla_{xy}^2 + \frac{n^2}{n_{in}^2}\right)U_n(x, y) = 2\xi_n U_n(x, y), \quad (4)$$

and $U_n(x, y) = 0$ on the edge of the cavity. Second, it is assumed that only two modes of slightly different

oscillation frequencies obtain positive gain. Then, the electric and polarization field can be expanded by these two modes [13,14],

$$\tilde{E}(x,y,t) = \sum_{n=1,2} E_n(t)\exp[-i(\nu_n t + \phi_n)]U_n(x,y), \quad (5)$$

$$\tilde{\rho}(x,y,t) = \sum_{n=1,2} p_n(t)\exp[-i(\nu_n t + \phi_n)]U_n(x,y), \quad (6)$$

where $E_n(t)$ is real while $p_n(t)$ is complex, and ν_n and ϕ_n are the frequency and the phase of the mode n, respectively.

We also assume that these two modes belong to different symmetry classes. Therefore we obtain the following important properties of the forth-order integrals:

$$\iint U_1 U_2^3\, dxdy = \iint U_1^3 U_2\, dxdy = 0. \quad (7)$$

Solving Eqs. (1)–(3) by a perturbational method [13,14] for the small electric field and using Eq. (7) yields the following equations:

$$\frac{dE_1}{dt} = (\alpha_0 W_\infty - \alpha_L)E_1 - \alpha_0\beta_0 W_\infty I_{22}E_1 E_2^2 \cos 2\Phi$$
$$- \alpha_0\beta_0 W_\infty(I_{40}E_1^2 + 2I_{22}E_2^2)E_1, \quad (8)$$

$$\frac{dE_2}{dt} = (\alpha_0 W_\infty - \alpha_L)E_2 - \alpha_0\beta_0 W_\infty I_{22}E_2 E_1^2 \cos 2\Phi$$
$$- \alpha_0\beta_0 W_\infty(I_{04}E_2^2 + 2I_{22}E_1^2)E_2, \quad (9)$$

$$\frac{d\Phi}{dt} = (\xi_1 - \xi_2) + \alpha_0\beta_0 W_\infty I_{22}(E_1^2 + E_2^2)\sin 2\Phi, \quad (10)$$

where $\Phi \equiv \nu_1 t + \phi_1 - \nu_2 t - \phi_2$, $\alpha_0 \equiv 2\pi N\kappa\hbar\tilde{\kappa}/\epsilon\tilde{\gamma}_\perp$, $\beta_0 \equiv 4\tilde{\kappa}^2/\tilde{\gamma}_\perp\tilde{\gamma}_\parallel$, and $I_{ij} \equiv \int U_1^i U_2^j dxdy$.

When W_∞ is large enough, Eqs. (8)–(10) have two stable fixed points $\Phi_{s,\pm} = \pm\pi/2 + \Psi$ corresponding to the stationary lasing states and two unstable fixed points $-\Psi, \pi - \Psi$ where $\nu_1 = \nu_2 = \Delta_0$ and

$$\Psi = \frac{1}{2}\sin^{-1}\left\{\frac{\xi_1 - \xi_2}{\alpha_0\beta_0 W_\infty I_{22}(E_{1,s}^2 + E_{2,s}^2)}\right\}. \quad (11)$$

Here

$$E_{1(2),s}^2 = \frac{-\alpha_L + \alpha_0 W_\infty - (I_{22}/I_{04(40)})(-\alpha_L + \alpha_0 W_\infty)}{\alpha_0\beta_0 W_\infty\left(I_{40(04)} - (I_{22}^2/I_{04(40)})\right)}. \quad (12)$$

Therefore, two modes belonging to the different symmetry classes can lase with the same locking frequency, and then the pattern of the lasing state becomes asymmetric.

In the case of the actual microcavities, the refractive index should be finite and the cavity modes are the resonances instead of the bound states. Therefore the nonlinear dynamical simulation for Eqs. (1)–(3) is neces-
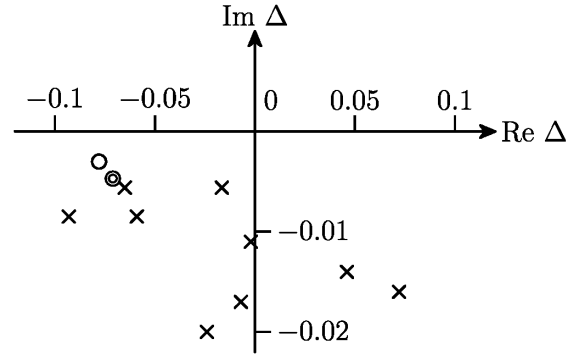

FIG. 1. Resonances of a microstadium cavity. The double and single circles correspond to the resonances of the maximum and second maximum gain.

sary to study the dynamics of two-mode lasing in 2D microcavities.

In our simulation we chose a stadium [15] for the cavity shape consisting of two half circles of the radius $R = 49/4\sqrt{2} \approx 8.75$ and two flat lines of the length $2R$ as shown in Fig. 2. We set the refractive index inside and outside the stadium $n_{in} = 2$ and $n_{out} = 1$, respectively. The other parameters are reported to be as follows: $\tilde{\gamma}_\parallel = 0.003$, $\tilde{\gamma}_\perp = 0.006$, $\epsilon = 4.0$, $\alpha_L = 0.004$, $N\kappa\hbar\omega_0 = 1.0\epsilon\tilde{\kappa} = 0.5$, $\Delta_0 = -0.07$.

The resonances obtained by the extended boundary element method [10,16] are shown in Fig. 1. The resonances denoted by the double circle and circle are close to the gain center $\Delta_0 = -0.07$ and have long lifetimes. We call them modes A and B, respectively. The wave functions of modes A and B corresponding to these resonances are shown in Figs. 2(a) and 2(b). Modes A and B belong to the different symmetry classes: Mode A belongs to $\psi_{--}(x,y)$ while mode B belongs to $\psi_{++}(x,y)$.

First let us explain single-mode lasing on mode A. As the pumping power W_∞ is increased more than $W_{sing} = 1.5 \times 10^{-4}$, the total light intensity inside the stadium grows exponentially and saturates to be a constant for arbitrary initial states. The wave function of the final stable state excellently corresponds to the wave function of mode A. Therefore, only mode A can lase in this region of W_∞.

Next we discuss two-mode lasing on modes A and B. Mode-pulling phenomena here can be classified into quasiperiodic behaviors of 2D tori and limit cycles. When W_∞ is increased more than $W_t = 1.9 \times 10^{-4}$, mode B also can obtain enough gain to lase. When $W_t < W_\infty < W_l = 1.0 \times 10^{-3}$, the interaction between modes A and B is small and hence the time evolution of the light field is quasiperiodic as if there exist two independent modes of different oscillation frequencies ν_1 and ν_2. As W_∞ is increased more than W_l, the interaction between modes A and B becomes larger. Consequently, the light field is attracted into a limit cycle. When $W_l < W_\infty < W_{lock} = 5.6 \times 1.0^{-3}$, the optical spectrum has two large peaks
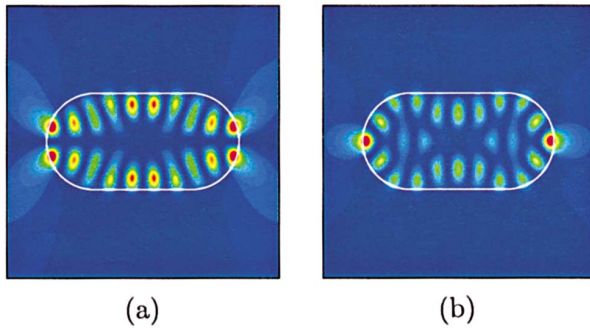
FIG. 2 (color). The wave function of the metastable resonance of (a) the double circle and (b) single circle in Fig. 1. These wave functions are solutions of the linear Schrödinger-Helmholtz equation. The symmetry classes of these modes are, respectively, (a) $\psi_{--}(x, y)$ and (b) $\psi_{++}(x, y)$. The white curve denotes the stadium cavity.

at ν_1 and ν_2, respectively, corresponding to modes A and B, and small peaks of their higher harmonics. The frequency difference $|\nu_1 - \nu_2|$ decreases as the pumping power increases, as shown in Fig. 3(a).

Finally we explain locking of modes A and B. When $W_\infty > W_{lock}$, the total intensity of the light field inside the cavity grows exponentially at first and shows the relaxation oscillation, and at last becomes stationary. The frequency difference $|\nu_1 - \nu_2|$ vanishes at $W_\infty = W_{lock}$ as shown in Fig. 3(a), and hence the optical spectrum has only one peak. The final stationary lasing state has an asymmetric pattern as shown in Fig. 3(b) in spite of the symmetric shape of the cavity.

We have thus far reported the dynamics of two-mode lasing in a 2D microcavity of the stadium shape. Here we emphasize that we checked the same route to the locking of two modes in the microcavities of elliptic and oval shapes. Therefore, we conclude that the dynamics of two-mode lasing described above is not unique for the stadium shape but universal for those 2D microcavity lasers which are symmetric with respect to the x and y axes.
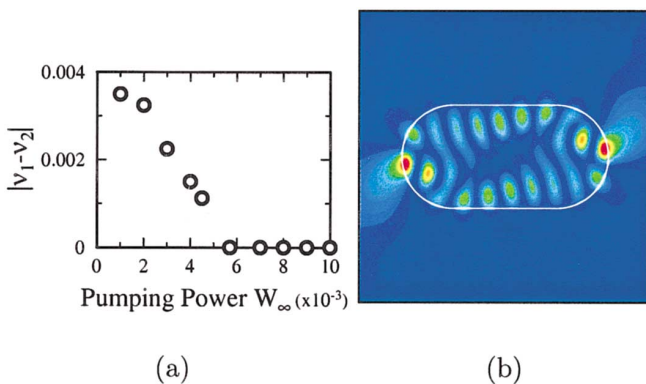

FIG. 3 (color). (a) The difference of the frequencies ν_1 and ν_2 corresponding to the two lasing modes decreases as the pumping power increases. (b) The asymmetric pattern of the final stable oscillation of the light field.
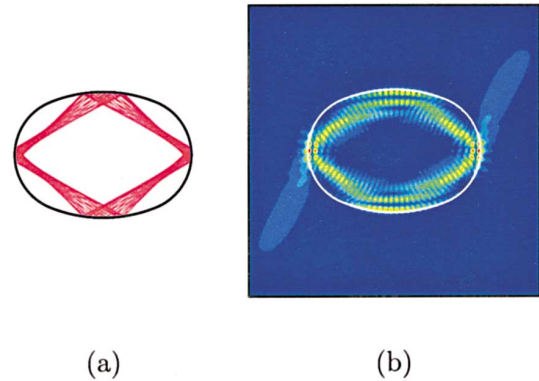

FIG. 4 (color). (a) A trajectory on the ring-type KAM torus in the oval billiard. (b) An asymmetric locking state associated with the ring-type KAM torus.

In the case of the oval-shaped cavity [17,18], there exists a stable periodic orbit of a ring type because it is a so-called mixed system. Accordingly, the trajectory around this closed ring trajectory forms a 2D torus called a Kol'mogorov-Arnol'd-Moser (KAM) torus as shown in Fig. 4(a). Linear wave mechanics gives us two resonances of different symmetry classes associated with this KAM torus [4,5,18]. The difference of their frequencies is very small, and hence they are easily locked to produce an asymmetric lasing pattern associated with the ring-type KAM torus as shown in Fig. 4(b).

In order to observe locking of two modes associated with the ring-type KAM torus, we actually fabricated the "quasistadium shape" microcavity laser diode by a molecular beam epitaxy-grown graded-index separate-confinement heterostructure single-quantum-well (GRIN-SCH-SQW)GaAs/AlGaAs structure and reactive ion etching as shown in Fig. 5 [19]. The cavity length L, the width W, and the radius R of the curved end mirrors are 600, 60, and 600 μm, respectively. Therefore, this quasistadium microcavity satisfies the *confocal* resonator condition. The sidewall mirrors are separated from both
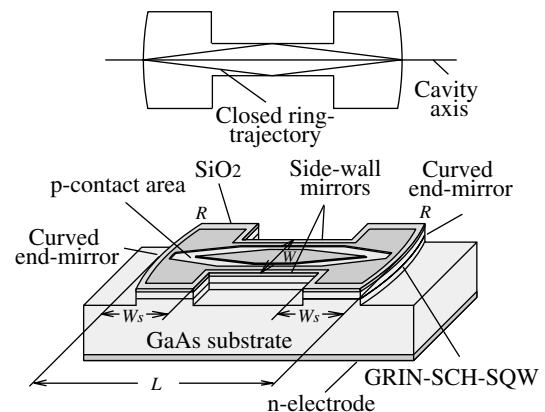

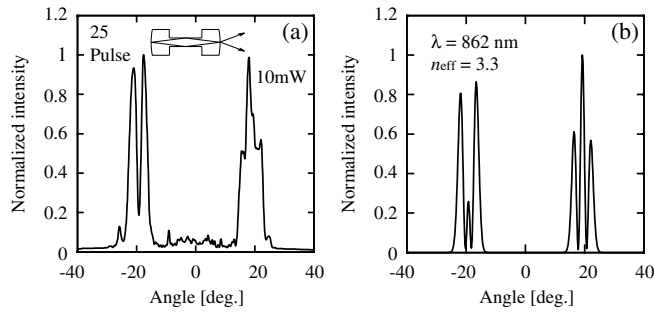FIG. 5. Schematic diagram of the confocal quasistadium laser diode.

FIG. 6. (a) Observed far field pattern at the output power of 10 mW. (b) Calculated far field pattern for the locking state of two modes associated with the ring-type KAM torus.

cavity ends by distance $Ws = 160$ μm. The p-contact area was formed along the closed ring trajectory shown in Fig. 5 in order to lase only the resonance modes associated with this trajectory.

A pulse current with 500 ns width and 1 kHz repetition was used for evaluation. Threshold current was evaluated to be 153 mA. The optical spectrum has a peak at the wavelength of 862 nm. Figure 6(a) shows the observed far field patterns at the output power of 10 mW. The origin of the angle corresponds to the cavity axis. The far field pattern shows highly directional emission in two directions which correspond to the closed ring trajectory. In addition, the far field pattern is asymmetric although the quasistadium is symmetric. The measurement of the far field pattern is very slow, and so this asymmetric pattern is stationary.

We calculated the resonance modes by the extended Fox-Li mode calculation method [20,21]. We found two resonance modes of slightly different frequencies around the observed wavelength 862 nm and different symmetry classes of $\psi_{++}(x, y)$ and $\psi_{+-}(x, y)$ that have low loss and localize on the closed ring trajectory. The Schrödinger-Bloch model is not applicable to this laser because of the lack of computational power. Therefore we just superposed these two modes and obtained the asymmetric pattern in Fig. 6(b) nicely corresponding to the observed pattern. Consequently, we conclude that we observed locking of two modes of different symmetry classes in the real experiment of the semiconductor microcavity laser diode.

Two-mode lasing in 2D microcavity may well find applications for modulation and switching in optical communications and integrated optical circuits.

[1] *Optical Processes in Microcavities*, edited by R. K. Chang and A. J. Campillo (World Scientific, Singapore, 1996).
[2] Y. Yamamoto and R. E. Slusher, Phys. Today **46**, No. 6, 66 (1993).
[3] J. U. Nöckel and A. D. Stone, Nature (London) **385**, 45 (1997).
[4] C. Gmachl, F. Capasso, E. E. Narimanov, J. U. Nöckel, A. D. Stone, J. Faist, D. L. Sivco, and A. Y. Cho, Science **280**, 1556 (1998).
[5] C. Gmachl, E. E. Narimanov, F. Capasso, J. N. Baillargeon, and A. Y. Cho, Opt. Lett. **27**, 824 (2002).
[6] M. Gonokami, K. Takeda, H. Yasuda, and K. Ema, Jpn. J. Appl. Phys. **31**, L99 (1992).
[7] S. L. McCall, A. F. J. Levi, R. E. Slusher, S. J. Pearton, and R. A. Logan, Appl. Phys. Lett. **60**, 289 (1992).
[8] J. Faist, C. Gmachl, M. Striccoli, C. Sirtori, F. Capasso, D. L. Sivco, and A. Y. Cho, Appl. Phys. Lett. **69**, 2456 (1996).
[9] C. Gmachl, J. Faist, F. Capasso, C. Sirtori, D. L. Sivco, and A. Y. Cho, IEEE J. Quantum Electron. **33**, 1567 (1997).
[10] T. Harayama, P. Davis, and K. S. Ikeda, Phys. Rev. Lett. **90**, 063901 (2003).
[11] T. Harayama, P. Davis, and K. S. Ikeda, Phys. Rev. Lett. **82**, 3803 (1999).
[12] T. Harayama, P. Davis, and K. S. Ikeda, Prog. Theor. Phys. Suppl. **139**, 363 (2000).
[13] M. Sargent, III, M. O. Scully, and W. E. Lamb, Jr., *Laser Physics* (Addison-Wesley, Reading, MA, 1974).
[14] W. E. Lamb, Phys. Rev. **134**, A1429 (1964).
[15] L. A. Bunimovich, Commun. Math. Phys. **65**, 295 (1979).
[16] J. Wiersig, J. Opt. A: Pure Appl. Opt. **5**, 53 (2003).
[17] G. Benettin and J. M. Strelcyn, Phys. Rev. A **17**, 773 (1978).
[18] H. Makino, T. Harayama, and Y. Aizawa, Phys. Rev. E **59**, 4026 (1999).
[19] T. Fukushima *et al.*, Opt. Lett. **27**, 1430 (2002).
[20] A. G. Fox and T. Li, Bell Syst. Tech. J. **40**, 453 (1961).
[21] T. Fukushima, J. Lightwave Technol. **18**, 2208 (2000).